FABRICATION AND TESTING OF DURABLE REDUNDANT AND FLUTED-CORE JOINTS FOR COMPOSITE SANDWICH STRUCTURES

Shih-Yung Lin, Scott C. Splinter, Chris Tarkenton, David A. Paddock, and Stanley S. Smeltzer
NASA Langley Research Center, Hampton, VA 23681-2199

Sayata Ghose[‡], Juan C. Guzman[‡], Donald J. Sutkus[*], and Douglas A. McCarville[‡]
[‡]The Boeing Company, Seattle, WA 98124-2207
[*]Mosley Technical Services, Huntsville, AL 35802

ABSTRACT

The development of durable bonded joint technology for assembling composite structures is an essential component of future space technologies. While NASA is working toward providing an entirely new capability for human space exploration beyond low Earth orbit, the objective of this project is to design, fabricate, analyze, and test a NASA patented durable redundant joint (DRJ) and a NASA/Boeing co-designed fluted-core joint (FCJ). The potential applications include a wide range of sandwich structures for NASA's future launch vehicles.

Three types of joints were studied − splice joint (SJ, as baseline), DRJ, and FCJ. Tests included tension, after-impact tension, and compression. Teflon strips were used at the joint area to increase failure strength by shifting stress concentration to a less sensitive area. Test results were compared to those of pristine coupons fabricated utilizing the same methods. Tensile test results indicated that the DRJ design was stiffer, stronger, and more impact resistant than other designs. The drawbacks of the DRJ design were extra mass and complex fabrication processes. The FCJ was lighter than the DRJ but less impact resistant. With barely visible but detectable impact damages, all three joints showed no sign of tensile strength reduction. No compression test was conducted on any impact-damaged sample due to limited scope and resource. Failure modes and damage propagation were also studied to support progressive damage modeling of the SJ and the DRJ.

1. INTRODUCTION

The development of durable bonded joint technology for assembling large composite structures was an essential component of future space explorations. This effort was geared to provide an entirely new capability for human space exploration beyond Earth orbit. Under a Space Act Agreement (SAA No. SAA1−1018 Annex 4), NASA and Boeing cooperated to design, fabricate, analyze, and test generic joints applicable to a wide range of composite sandwich structures.

Three joint types were investigated: SJ, DRJ (NASA patent pending, [1]), and FCJ (a NASA/Boeing invention, [2]). Figure 1illustrates the joint configurations. To establish a baseline of strength and stiffness, pristine samples without a joint were added to the test matrix. While the joint types were generic, design and fabrication of the samples were geared toward potential applications for large space structures.
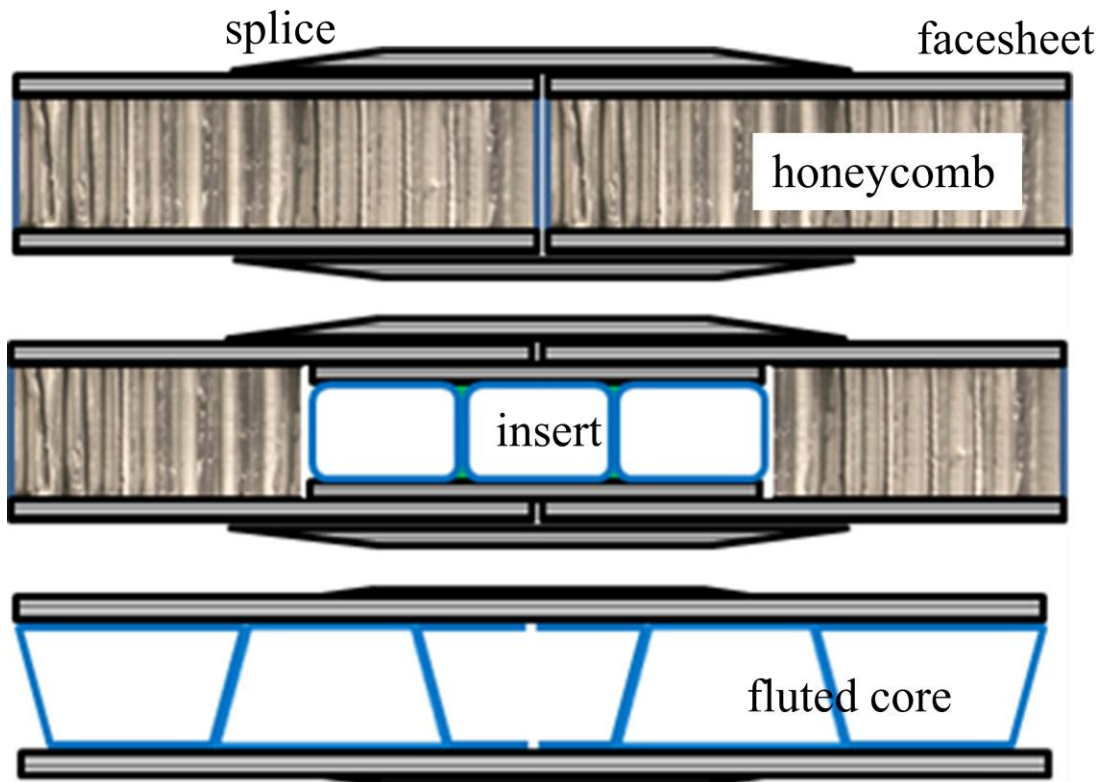
Figure 1   SJ, DRJ, and FCJ

Tests conducted include:

- tension, to determine tensile failure strength, failure modes, and post failure behaviors; some with a barely visible but detectable impact damage;
- compression, to determine compressive failure strength, failure modes, and buckling behaviors.

There were two additional efforts closely related to this work. Girolamo [3] focused on the joint adhesive fracture properties and Leone et al. [4] on the Progressive Damage Analysis (PDA) of joints. Both shall be referenced to paint a complete picture of joint failure behaviors.

2. DESIGN AND FABRICATION

Three composite sandwich panel joints were designed. The SJ had a honeycomb core. The DRJ had an insert and a honeycomb core. The FCJ had trapezoidal-shaped core along the length of the panel. The SJ was considered a baseline, to which data from the other two panel joints were compared. The DRJ was a heavier and stronger splice joint design developed by NASA to withstand impact damages. The FCJ was originally a Boeing design [5], initially called a "DC" joint after its originators. The FCJ represented a further evolution of the DC joint, redesigned by the NASA/Boeing team, to decrease mass and to develop an out-of-autoclave fabrication process.

2.1 Design Features

Designs were geared toward applications for lightly-loaded minimum-gauged large composite space structures. Basic construction of SJ and DRJ samples was 25.4mm thick honeycomb core (HexWeb™ CRIII–1/8–5052–.0007P–3.1 perforated, [6]) with two six-ply facesheets. The facesheet material was made of grade 190 TE–1 tapes (toughened epoxy/T800). The stacking sequence was [60°/ 0°/ -60°]s with the 0° direction transverse to the proposed joint orientation. The facesheets were bonded to the honeycomb core using FM 300–M film adhesive. Fluted-core samples had the same 25.4mm core thickness, but the facesheets were made of T800S/5320–1 and bonded with FM 209-1 adhesive for out-of-autoclave processes.

The interleaved ply-drop configuration with 6.35mm between ply-drops was selected for the splices (Figure 2). Another design feature added to the SJ and DRJ was a 6.35mm wide Teflon® strip running the length of the joint, located at the edge of each panel. This feature was integrated based on previous related work [4] to characterize the effects of the Teflon® (PTFE) strip on the joint through a PDA study. The intended function of this strip was to shift stress concentrations associated with edge effects of the joined panels, to a less critical location.
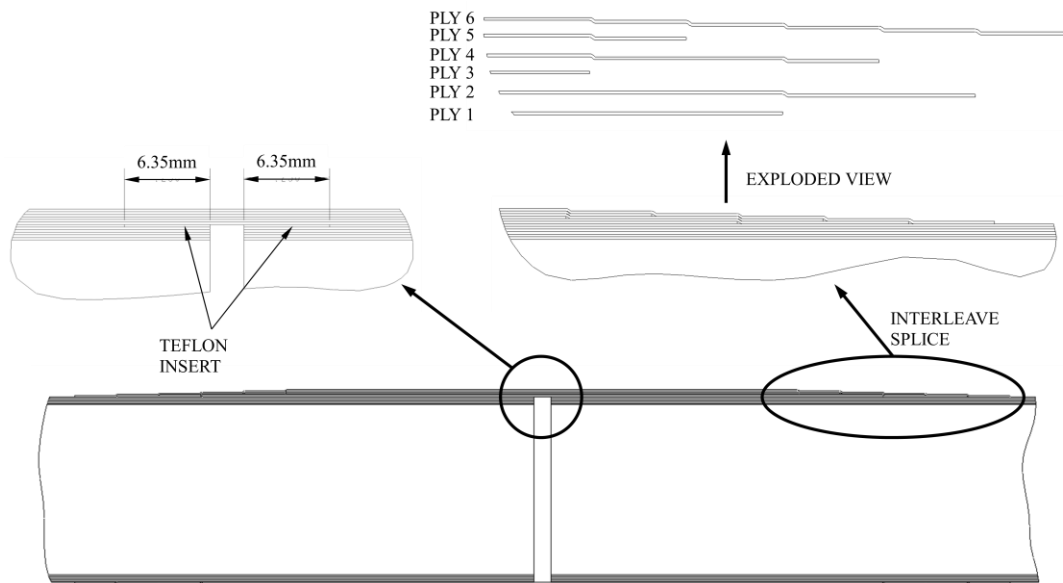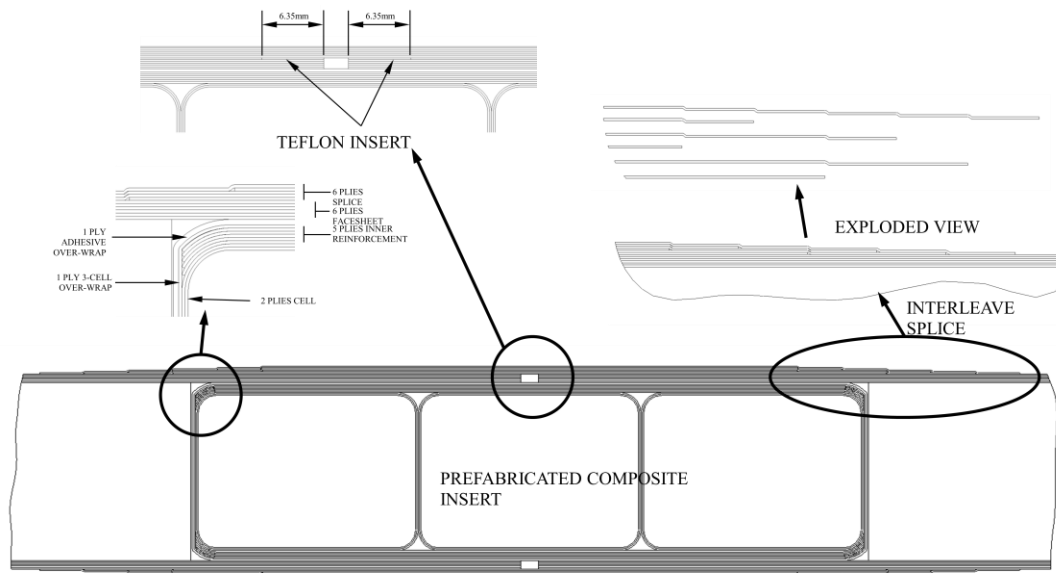

Figure 2   SJ with Teflon® edge relief strip and interleaved ply-drop scheme

2.1.1 Durable Redundant Joint (DRJ)

The DRJ (Figure 3) represented an enhancement to standard SJ configurations. In the region near the joint, the honeycomb material was removed. A separate prefabricated composite insert was placed in this region spanning the two panels to be joined. Three identically shaped, rectangular mandrels were wrapped with two plies oriented ±45° to form cells. Six plies were laid-up above and below the cells in the sequence of [60°/ 0°/ -60°]s with the outermost 60° ply wrapped around all three mandrels to create a single unit. Unidirectional radius fillers were inserted in the gaps formed by the spaces between the cells' corners. Prior to placement of the DRJ insert into the core cavity of each joined panel, a layer of FM300–M was wrapped around the insert. The interleaved splice was then bonded and then autoclave cured on top of the facesheets to finish the joint, including the addition of the Teflon® strips.

Figure 3   DRJ with prefabricated composite insert, Teflon® edge relief strip and interleaved ply-drop scheme

2.1.2 Fluted-Core Joint (FCJ)

The fluted core panel design (Figure 1) represents an alternative to honeycomb core, with potential mass reduction. The design for this configuration, initially conceptualized by researchers at Boeing, went through numerous iterations, including a reevaluation of the manufacturing process, material selection, and joint design. Individual, two-ply wrapped mandrels were laid-up using toughened epoxy pre-pregs, with a stacking sequence of [±45°]. Lay-up was done in an alternating pattern and cured in an autoclave process to form the "flutes." Unidirectional radius fillers were inserted in the gaps formed by the spaces between the flutes' corners, similar to the DRJ. Facesheets made of T800S/5320–1 pre-preg were placed on the cured flutes in a stacking sequence of [60°/ 0°/ -60°]s with the 0°-direction transverse to the axis of the flutes. FM 209–1 (instead of FM 300–M) adhesive, for out-of-autoclave (OoA) cure, was used to bond the facesheets to the fluted core.

The FCJ panel was identical in construction to the pristine fluted-core panel except for the addition of two "splice" plies interleaved into each facesheet. These two splice plies were to be placed where the two core panels were joined. Because of their sensitive nature, the details of the joint are not illustrated here.

2.2 Fabrication

Table 1 lists the relative masses of samples with and without joints for comparison. For areas outside of a joint, fluted-core is 16 percent heavier than honeycomb. At the joint, the DRJ is heavier and the FCJ is lighter compared to the SJ.

Table 2 lists the materials used and their purposes. All of them are commercially available. Table 3 lists the process parameters chosen for sample preparations.

Table 1   Mass comparison of joints, 0.140m (5.5") wide section

Sample Type	Mass (kg/m)	Normalized
Honeycomb, no joint	0.659	1.00
Flute-core, no joint	0.782	1.16
SJ	1.045	1.55
DRJ	1.494	2.17
FCJ	0.850	1.26

Table 2.   List of materials and their purposes.

| Material	Purpose
5320–1/T800 out of autoclave tape, 24" wide (Cytec)	Fabrication of out-of-autoclave sections
Grade 190 TE–1 tape (toughened epoxy/T800), 6" or 12" wide (Toray)	Fabrication of autoclave sections
FM300–M adhesive (Cytec)	Adhesion of autoclaved sections
FM209–1 adhesive (Cyrec)	Adhesion of out-of-autoclaved sections
CG1305 A+B (Huntsman Advanced Materials) as the potting compound	Fill any hollow spaces of samples at the load application sections
Polyester peel ply (Precision Fabric)	For material curing process
Glass fiber preimpregnated epoxy resin for making the tabs	Sample tabs for load applications
Aluminum Honeycomb Core—CRIII–1/8–5052–.0007P–3.1	Core of honeycomb panels
EA9394 paste adhesive (Henkel)	Attach glass tabs
Aluminum 2024-T3, 0.063" thick	Double cantilever beam sample doubler

Table 3.   Component process parameters.

Component	Process Parameters
Honeycomb panel	Autoclave for 2 hours at 350° F under 45 psi with a vent at 20 psi per Boeing processing specification HBPS–22–006
SJ, DRJ, Fluted-core	Autoclave for 2 hours at 350° F, under 85 psi pressure
Fluted-core panel, FCJ	Out-of-autoclave, Boeing proprietary

3. EXPERIMENTATION

Tension tests were configured as illustrated in Figure 4. Strain gages, displacement gages, video image correlation systems (VIC 3D), digital cameras and video cameras were used to make measurements and/or observations. Compression tests had similar configuration except for a test stand with flat loading platens. As illustrated in Figure 5, there were four alignment gages outside of joint area to ensure proper loading and measure strains at their locations. Two rosettes were installed in the joint area.
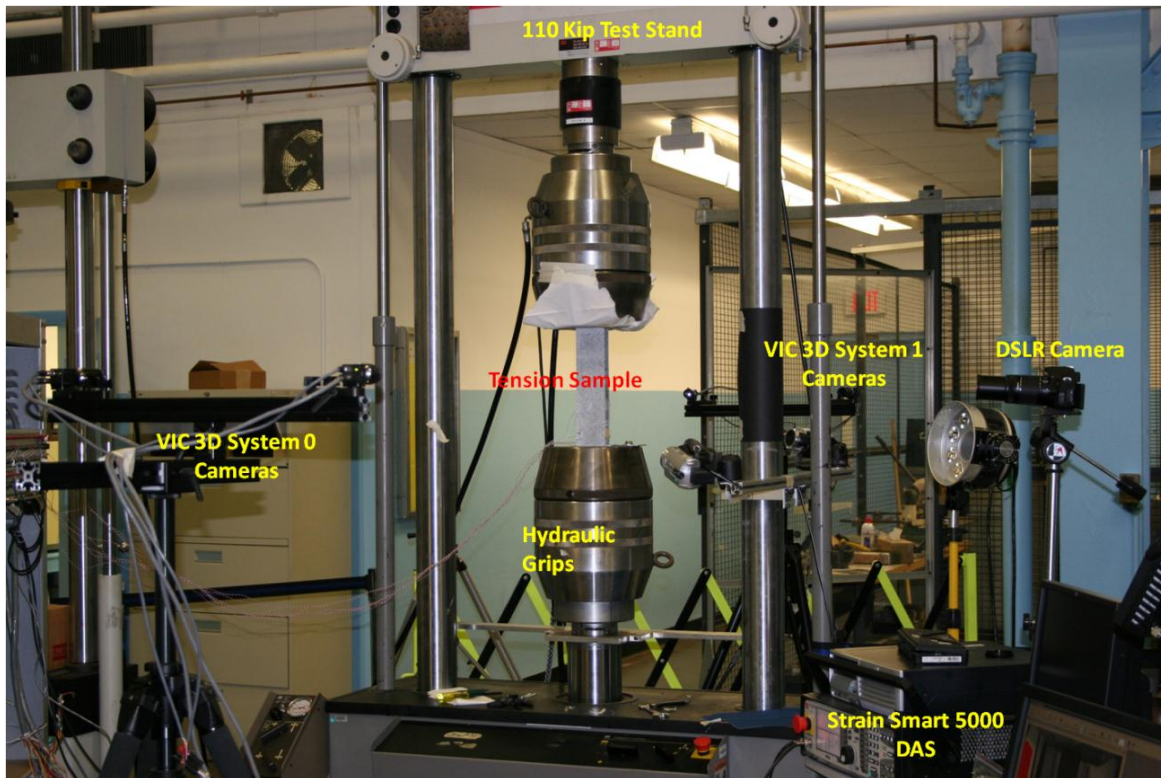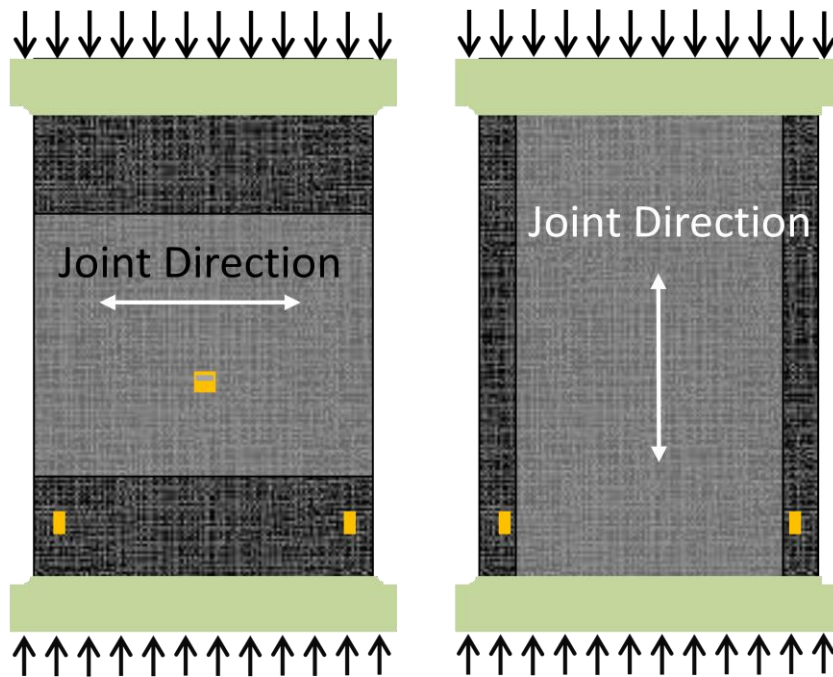

Figure 4   Tension test setup
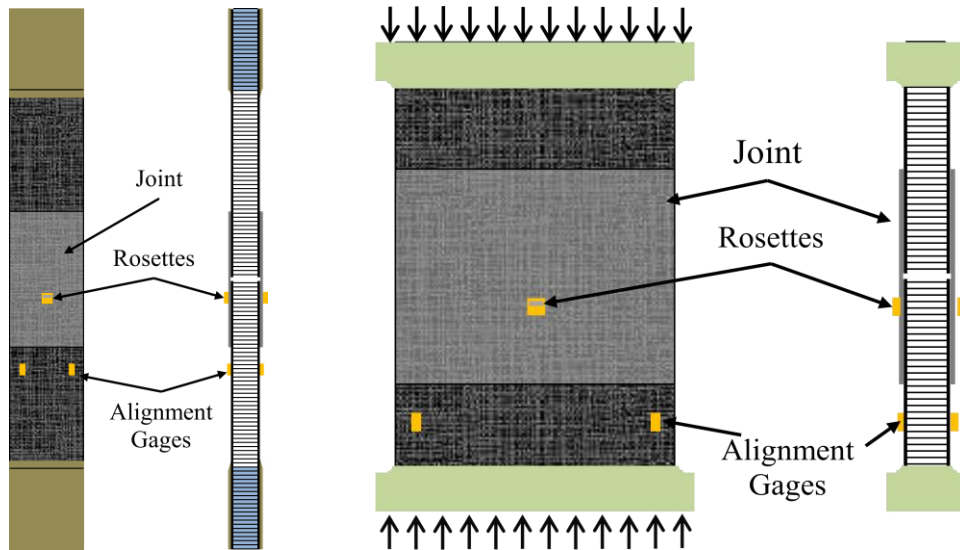
Figure 5   Tension and compression test strain gage patterns

Compression tests of the joints were conducted in both directions: loaded perpendicular and parallel to joints as illustrated in Figure 6.

Figure 6   Compression tests loaded in perpendicular and parallel to joint directions

4. RESULTS

Table 4 lists the failure loads and strain gage data of all the tests. Unfortunately, the pristine tension samples all failed too close to the grip and were considered invalid.

4.1 SJ Tensile Test

SJ tension tests failed at the joint as predicted by PDA [4] and FEA [7]. However, the damage propagation involved core crushing that was not expected initially. As shown in Figure 7, the Teflon® tape in the joint design initiated the crack propagation as expected. The load changed direction while transitioning from facesheet to splice introduced a bending moment compressing the core. Because of the light gauge core being used, the core was crushed at two-thirds of the failure load of the joint. This allowed extra deformation of the facesheet away from the already separated splice and allowed mode I fracture propagation at the delamination front. Since FM 300M adhesive is tougher than the composite material used as discussed in [3], the delamination quickly transitioned into the splice between the 0 and 60 degree plies. Finally the splice was broken off, causing total separation at the joint.

The core crush phenomenon reduced SJ failure strength according to PDA [4]. Reinforcement of the core with additional crush support or using a heavier gauge core at the joint may improve the strength. That line of research was left for future efforts to study.

Table 4   Test Results

Sample	Test	Failure Load (kN)	Failure Strain (µε)	Failure Strain at Joint (µε)
SJ	Tension	110.6	11,707	9,712
SJ Impact	Tension	107.7	11,098	
DRJ	Tension	135.2	14,136	4,689
DRJ Impact	Tension	135.7	14,169	
Fluted Core Pristine	Tension	123.5	12,627	
FCJ	Tension	123.9	9,948	12,906
FCJ Impact	Tension	121.5	9,704	
Pristine Honeycomb	Compression	-100.3	-5,338	
SJ, transverse	Compression	-104.9	-5,561	-2,661
SJ, longitudinal	Compression	-233.6	-7,358	
DRJ, transverse	Compression	-109.1	-5,407	-1,452
DRJ, longitudinal	Compression	-324.4	-7,214	
Fluted Core Pristine Transverse	Compression	-9.3	-1,427	
Fluted Core Pristine, longitudinal	Compression	-307.7	-7,793	
FCJ, transverse	Compression	-10.0	-1,853	
FCJ, longitudinal	Compression	-204.2		
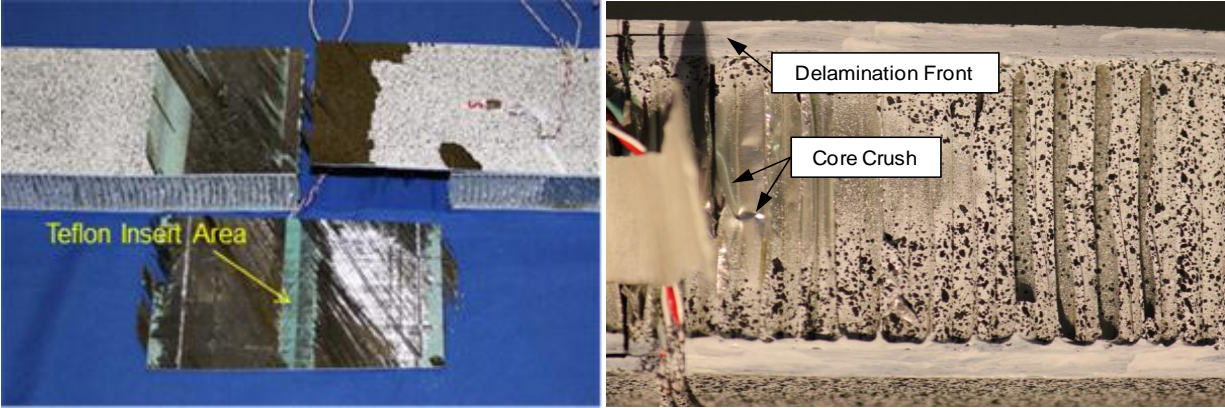
<table>
<tr><td>(a) Failure surfaces.</td><td>(b) Delamination and core crush.</td></tr>
</table>

Figure 7   SJ tension failure behaviors.

4.2 DRJ Tension Test

The DRJ also failed at the joint. The failure started at just outside of the corners of the insert with minor delamination. At the later stage of the test, only one of the two samples displayed separation at the Teflon® insert. Therefore, the Teflon® strip in the DRJ was not believed to have much contribution to the failure strength as did the Teflon® strip in the SJ.   The insert was able to share tensile load and reduced bending in the load path. No crushing of the web was observed. Final failure happened quickly with the facesheet pulling out between the splice and the insert. Figure 8 illustrates this phenomenon. The failure load was 22 percent higher than that of the SJ.
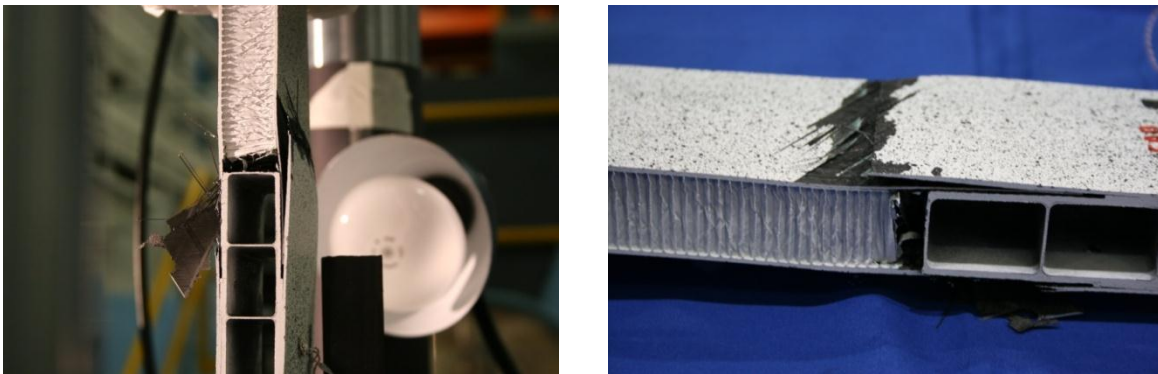

Figure 8   DRJ failure behaviors, facesheet pulled out from between the splice and the insert

4.3 FCJ Tension Test

The FCJ did not fail at the joint. Failure loads (12 percent higher than that of the SJ) and failure modes were similar with and without a joint. However, these samples exhibited very complex damage propagation behavior because of their design. First, the sample was not straight. When gripped, one side of the sample was partially buckled, as shown on the left side of Figure 9, due to bending moment introduced.
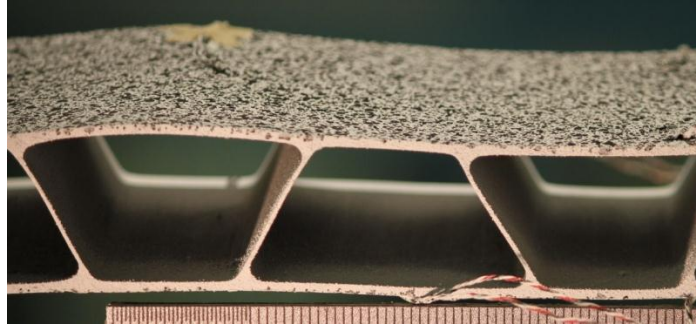
Figure 9   Fluted core sample gripped before loading.

Second, due to the geometry of the web, the load transferred between the front and back sides quite easily. Delamination at the webs, as shown in Figure 10, also complicated the load distribution.

Third, because damage propagation at one side caused that side to lengthen, the other side had to carry more load and eventually developed more damage and lengthened too. This process happened multiple times, and a large delamination area was developed before final failure with the facesheet on one side totally broken. As shown in Figure 10 : (a) shows delamination started at the left side, (b) shows extensive delamination and most of the load should be carried by the right side facesheet, (c) shows delamination developed on the right side and some web area separation, (d) shows extensive delamination on both sides, and then finally (e) shows final failure.


Figure 10.   Fluted core tension test, damage propagation.

Fourth, the alignment gages never worked in this design due to core geometry. Gage readings from all the fluted core tests scattered significantly more than other joint types. As shown in Figure 11, the VIC 3D strain pattern of FCJ is quite inconsistent compared to that of the SJ.

Figure 12 shows the VIC-3D pattern of a FCJ sample under compressive load just before failure. Local buckling was observed.
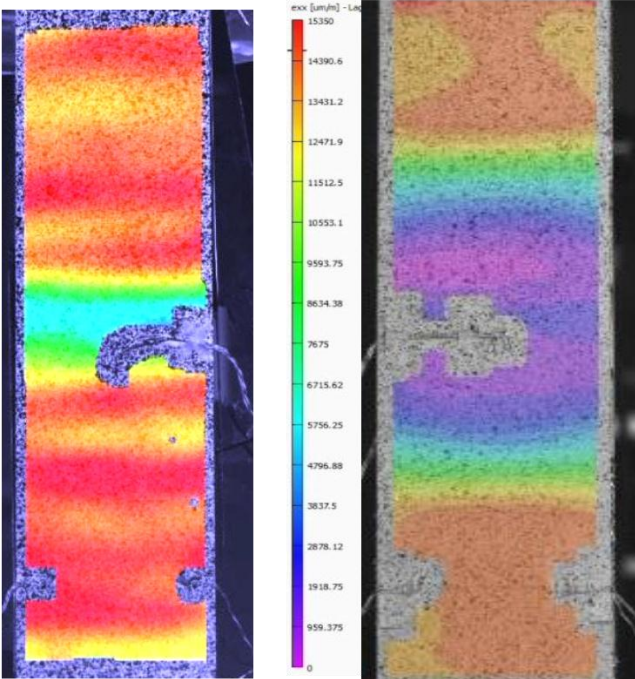
Figure 11. VIC 3D strain pattern in loading (vertical) direction. Left shows FCJ influenced by the core and right shows SJ having a more consistent pattern
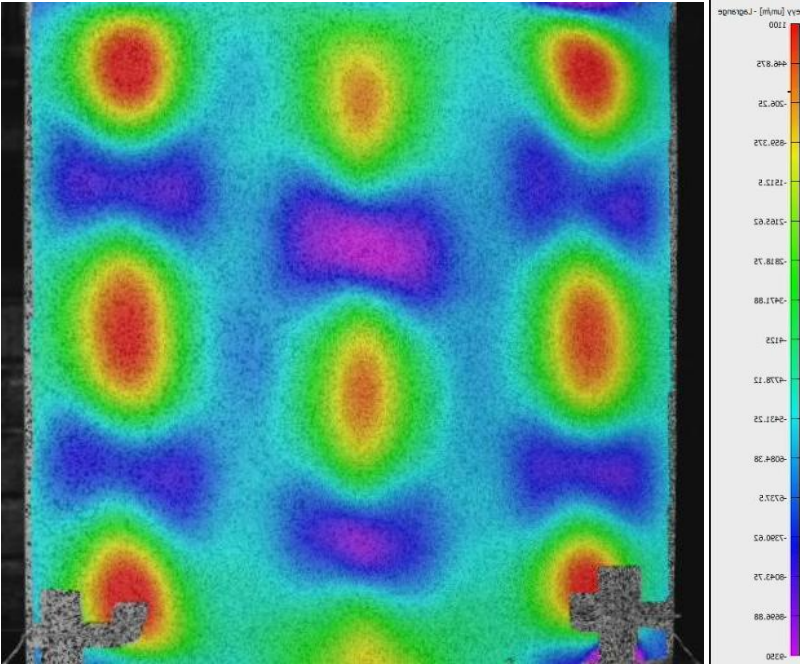
Figure 12   Vertical surface strain pattern on a FCJ compression sample

4.4 Tension Test with Impact Damage

Barely visible but detectable impact damage was introduced to the joints. Delamination sizes detected by ultrasound were within 25.4 to 50.8 mm as shown in Figure 13. Impact energy levels were adjusted to 0.339, 1.017, and 0.170 N·M according to joint design and impact damage resistance. Test results showed no difference in tensile strength as listed in Table 4.
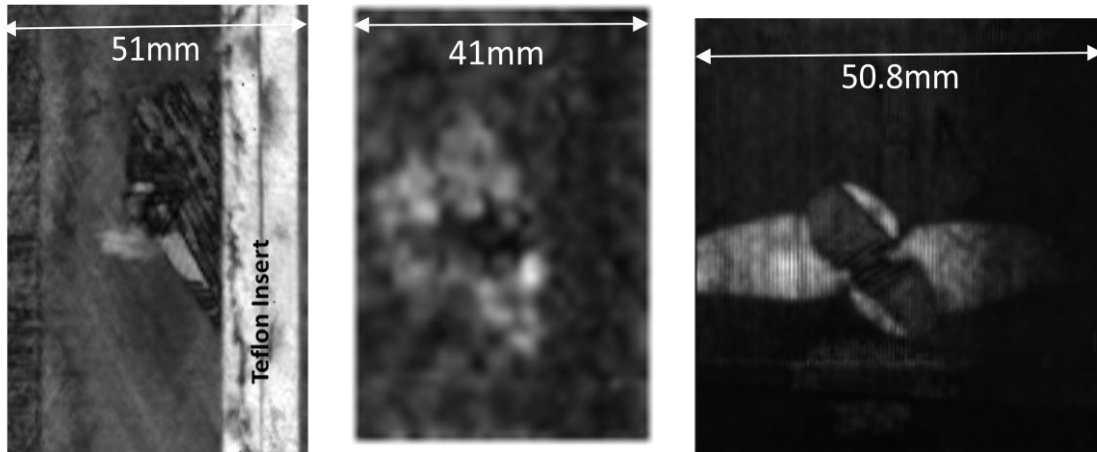

Figure 13   Impact damages at SJ, DRJ, and FCJ with 0.339, 1.017, and 0.170 N·M energy respectively

4.5 SJ and DRJ Compression Test

When tested perpendicular to joint direction, the SJ and the DRJ compression strengths showed no difference from the pristine panel.   The failure sites were always outside of the joint area. However, when tested parallel to the joint direction, the failure loads increased by a proportion greater than the corresponding increase in cross sectional area. The failure strain increased from -5400 to –7300 $\mu\varepsilon$. The cause of this change could be a stability issue with a thin net cross section. When tested perpendicular to joint direction, a sample could be more prone to be affected by minor defects in the panel. Figure 14 shows the failure mode.
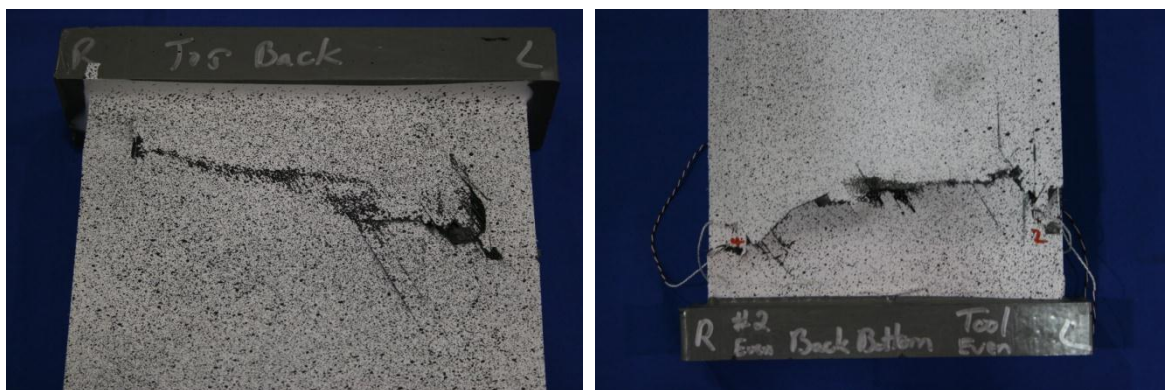

Figure 14.   Compression failure of SJ and DRJ loaded along the joint direction.

4.6 Fluted-core Compression Test

Tests conducted perpendicular to the joint direction, with and without a joint, had low buckling resistance due to its design. These samples came with some waviness due to their fabrication process, up to 0.9 mm between peak and valley according to surface profile measurements conducted separately. The samples were loaded to 56238 N/M (321 lbf/inch) when excessive lateral deflection was observed. Figure 15 shows the mode shape of a buckled sample.

Figure 15.   Buckling of a fluted core sample.

When tested in the perpendicular direction, with and without a joint, the compression strength and failure mode differed, unlike that of the tension tests. First, the failure strength dropped from 307.8 kN (69,186 lbf) pristine to 204.3 kN (45,918 lbf) with a joint. From the pictures in Figure 16 and Figure 17, one can clearly identify that the pristine sample suffered crushing on both sides while the one with a joint suffered crushing on one side and delamination/buckling on the other side. Even though some theories were developed to explain the differences, the root cause needs to be studied with additional efforts.
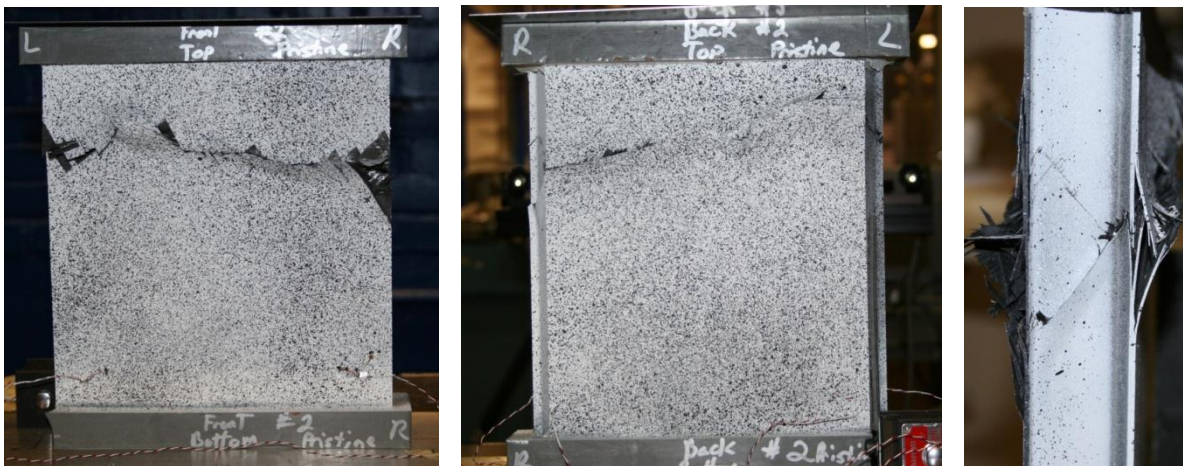

Figure 16.   Failure of pristine fluted core compressions sample; front, back, and side
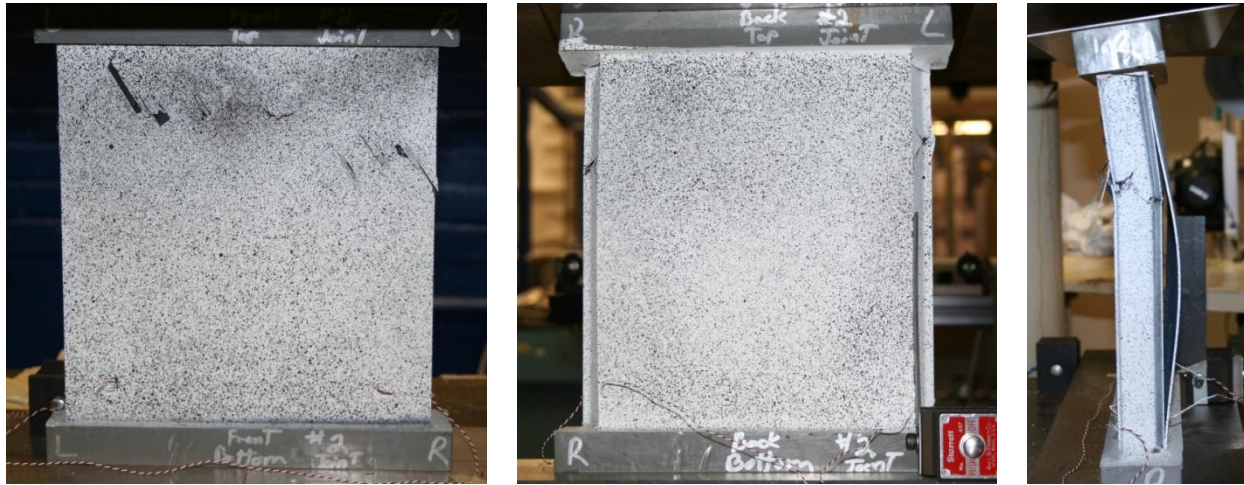
Figure 17.   Failure of FCJ compression sample; front, back, and side

5. CONCLUSIONS

This project set out to develop and test joint concepts for large composite space structures. Additional reports ([3], [4], and [7]) documented this effort with much greater detail. In the process, the knowledge and expertise in the field were expanded. The most notable conclusions were:

- Design details of three joints were earnestly discussed and implemented. The SJ was tested as baseline. The DRJ and the FCJ were manufactured and tested for the first time. The FCJ was also a new invention incorporating out-of-autoclave fabrication processes.
- Progressive damage mechanisms leading to the failure of the SJ were clearly identified with test instrumentation.
- Core crush phenomenon was observed in the tests and incorporated into the PDA to improve the accuracy of prediction. This also helped in understanding the risk of using light gage honeycomb core and to find the proper solution to mitigate the issue.
- Joint strength was tested and documented. Joint masses were compared.
- Impact damage effects were evaluated. A small detectable defect would not reduce the tensile strengths of these three joints.

This effort only tested and analyzed joints with minimum gage facesheet (6-ply) and the lightest honeycomb core. However, the knowledge base could be used to study different design parameters and applications.

6. REFERENCES

1. "Systems, methods, and apparatus for increasing durability of adhesively bonded joints in a sandwich structure," US Patent Application (US 2012/0034408 A1) Stanley S. Smeltzer, III; Eric C. Lundgren

2. Boeing/NASA Invention Disclosure 12-1346, 2012

3. "Progressive Damage Analysis of Composite Bonded Joints," Girolamo D.; MSc Thesis. TU Delft. December 2012

4. "Progressive Damage Analysis of Composite Sandwich Joints," Frank A. Leone, Donato Girolamo, Carlos G. Dávila, NASA TM 2012-217790

5. "Method for Joining Sandwich Truss Core Panels and Composite Structures Produced Therefrom," US Patent (US 2012/0090265 A1); Douglas A. McCarville, Juan C. Guzman, Michael Leslie Hand

6. "HexWebTM Honeycomb Attributes and Properties," HEXCEL® Composites, November 1999

7. "Durable Bonded Composite Joint Technologies", Shih-Yung Lin, Chris Tarkenton, Sayata Ghose, Frank Leone, NASA TM xxxx-xxxxxx in press